

H₂ Ejection from Polycyclic Aromatic Hydrocarbons: Infrared Multiphoton Dissociation Study of Protonated 1,2-Dihydronaphthalene

Martin Vala,^{*,†} Jan Szczepanski,[†] Jos Oomens,[‡] and Jeffrey D. Steill[‡]

Department of Chemistry and Center for Chemical Physics, P.O. Box 117200, University of Florida, Gainesville, Florida 32611-7200, and FOM Institute for Plasma Physics "Rijnhuizen", Edisonbaan 14, NL-3439MN Nieuwegein, The Netherlands

Received November 14, 2008; E-mail: mvala@chem.ufl.edu

Abstract: 1,2-Dihydronaphthalene (DHN) has been studied by matrix isolation infrared absorption spectroscopy, multiphoton infrared photodissociation (IRMPD) action spectroscopy, and density functional theory calculations. Formed by electrospray ionization, protonated 1,2-dihydronaphthalene was injected into a Fourier transform ion cyclotron resonance mass spectrometer coupled to an infrared-tunable free electron laser and its IRMPD spectrum recorded. Multiphoton infrared irradiation of the protonated parent (m/z 131) yields two dissociation products, one with m/z 129 and the other with m/z 91. Results from density functional theory calculations (B3LYP/6-31++G(d,p)) were compared to the low-temperature matrix isolation infrared spectrum of neutral DHN, with excellent results. Calculations reveal that the most probable site of protonation is the 3-position, producing the trihydronaphthalene (THN) cation, 1,2,3-THN⁺. The observed IRMPD spectrum of vapor-phase protonated parent matches well with that computed for 1,2,3-THN⁺. Extensive B3LYP/6-31G(d,p) calculations of the potential energy surface of 1,2,3-THN⁺ have been performed and provide insight into the mechanism of the two-channel photodissociation. These results provide support for a new model of the formation of H₂ in the interstellar medium. This model involves hydrogenation of a PAH cation to produce one or more aliphatic hydrogen-bearing carbons on the PAH framework, followed by photolytic formation and ejection of H₂.

Introduction

Polycyclic aromatic hydrocarbons (PAHs) are thought to be responsible for a number of spectral observations originating from the interstellar medium. They have been proposed as the carriers of the unidentified interstellar infrared (UIR) emission bands, a set of infrared peaks at 3.3, 6.2, 7.7, 8.6, 11.3, and 12.7 μm ,^{1,2} as well as responsible for the diffuse interstellar absorption bands (DIBs), a set of more than 200 bands observed in the visible spectral region.^{3–5} Recently, several reports have also proposed that PAHs may act as catalysts in the formation of H₂.^{6–9}

Although the main UIR peak in the 3.3 μm region has been attributed to the aromatic C–H stretching vibrations in PAHs, other weaker features, particularly at 3.4 μm , are believed to

result from aliphatic C–H stretching modes from either aliphatic side groups^{10–13} or extra hydrogen atoms attached directly to an aromatic ring.^{14,15} A number of groups have calculated that the addition of an H atom to a PAH cation is exothermic with no activation barrier.^{8,9,16,17} Ricca et al. have further demonstrated that there are no, or only small, activation barriers to the addition of multiple H atoms to naphthalene cations and that the preference is for addition on adjacent carbons.¹⁷ Using a flowing afterglow-selected ion flow tube apparatus, LePage et al. studied H atom attachment to benzene, naphthalene, and pyrene cations.¹⁸ Several groups have investigated whether protonated PAHs could account for some of the observed features of the UIR bands. Banisaukis et al. studied

[†] University of Florida.

[‡] FOM Institute for Plasma Physics "Rijnhuizen".

- (1) Leger, A.; Puget, J. L. *Astron. Astrophys.* **1984**, *137*, L5–L8.
- (2) Allamandola, L. J.; Tielens, A. G. G. M.; Barker, J. R. *Astrophys. J.* **1985**, *290*, L25.
- (3) Leger, A.; d'Hendecourt, L. *Astron. Astrophys.* **1985**, *146*, 81–85.
- (4) Crawford, M. K.; Tielens, A. G. G. M.; Allamandola, L. J. *Astrophys. J.* **1985**, *293*, L45–L48.
- (5) Salama, F.; Galazutdinov, G. A.; Krelowski, J.; Allamandola, L. J.; Musaev, F. A. *Astrophys. J.* **1999**, *526*, 265.
- (6) Bohme, D. K. *Chem. Rev.* **1992**, *92*, 1487–1508.
- (7) Cassam-Chenai, N. P.; Pauzat, F.; Ellinger, Y. *AIP Conf. Proc.* **1994**, *312*, 543.
- (8) Bauschlicher, C. W. *Astrophys. J.* **1998**, *509*, L125–L127.
- (9) Hirama, M.; Tokosumi, T.; Ishida, T.; Aihara, J. *Chem. Phys.* **2004**, *305*, 307–316.

- (10) de Muizon, J.; d'Hendecourt, L. B.; Geballe, T. R. *Astron. Astrophys.* **1990**, *235*, 367–378.
- (11) Joblin, C.; Tielens, A. G. G. M.; Allamandola, L. J.; Geballe, T. R. *Astrophys. J.* **1996**, *458*, 610–620.
- (12) Duley, W. W.; Grishko, V. I.; Kenel, J.; Lee-Dadswell, G.; Scott, A. *Astrophys. J.* **2005**, *626*, 933–939.
- (13) Sloan, G. C.; Bregman, J. D.; Geballe, T. R.; Allamandola, L. J.; Woodward, C. E. *Astrophys. J.* **1997**, *474*, 735–740.
- (14) Schutte, W. A.; Tielens, A. G. G. M.; Allamandola, L. J. *Astrophys. J.* **1993**, *415*, 397–414.
- (15) Bernstein, M. P.; Sandford, S. A.; Allamandola, L. J. *Astrophys. J.* **1996**, *472*, L127–L130.
- (16) Jolibois, F.; Klotz, A.; Gadea, F. X.; Joblin, C. *Astron. Astrophys.* **2005**, *444*, 629–634.
- (17) Ricca, A.; Bakes, E. L. O.; Bauschlicher, C. W. *Astrophys. J.* **2007**, *659*, 858–861.
- (18) Le Page, V.; Keheyan, Y.; Snow, T. P.; Bierbaum, V. M. *Int. J. Mass Spectrom.* **1999**, *185*, 949–959.

the effect of hydrogenation on the acenaphthylene cation and found that sequential hydrogen addition can occur even in cryogenic matrices.¹⁹ Beegle et al. reported that neutral hydrogenated naphthalene and pyrene give rise to enhanced intensity of the 6.2 μm band.²⁰ Lorenz et al. showed that gas-phase protonated naphthalene exhibits IR bands consistent with the UIR bands.²¹

The formation of the most abundant molecule in the interstellar medium, H₂, has long been thought to form by combination of hydrogen atoms on the surface of small dust grains.^{22–24} Recently, however, several groups have suggested that PAHs could act as reaction centers (i.e., catalysts) for the formation of H₂.^{6–9} This idea, first proposed by Bohme,⁶ was subsequently expanded upon by Cassam-Chenai et al.,⁷ Bauschlicher,⁸ and Hirama et al.,⁹ who independently reported calculations on a number of PAHs, including hydrogenated benzene, naphthalene, anthracene, pyrene, and coronene. The latter authors showed that the addition of the first H atom to a PAH cation is exothermic and that the abstraction of this H by a second incoming H to yield H₂ proceeds with a zero or only a small activation barrier, permitting the reaction to proceed at very low temperatures. Joblin and co-workers investigated another pathway for H₂ formation, the reaction of two hydrogens on nearby carbons followed by their bonding and removal, but calculated that this route, at least in naphthalene, has a higher barrier than sequential H atom ejection.¹⁶

In this paper, we report our spectroscopic study of 1,2-dihydronaphthalene (1,2-DHN), an atypical PAH (indeed not really a polycyclic aromatic hydrocarbon, but derived from one) containing two adjacent aliphatic carbons. This molecule was chosen for study because it is an example of a simple hydrogenated PAH whose study might provide insights into the contributions of such a molecule to the UIR bands and into the mechanism of H₂ formation using a PAH as a reaction center.

Neutral 1,2-DHN and its derivatives have been the subject of a number of experimental and theoretical studies for over 30 years^{25,26} because of its interesting photochromic properties. Very recently, Tomasello et al.²⁷ reported an in-depth theoretical study on the photochemical ring-opening in 1,2-DHN.

In the present paper we have used matrix isolation Fourier transform (FT) infrared spectroscopy to record the infrared spectrum of neutral 1,2-DHN (in Ar at 12 K) and, in addition, used a free electron infrared laser in conjunction with a FT ion cyclotron mass spectrometer with an electrospray source to determine the infrared multiphoton dissociation (IRMPD) spectrum of gas-phase protonated 1,2-DHN. Density functional theory calculations on neutral 1,2-DHN, possible structures for

the protonated DHN species, their vibrational spectra, and probable dissociation pathways are also reported.

Experimental Methods

Matrix Isolation Infrared Spectroscopy. The experimental apparatus used for the matrix study was similar to that described previously.²⁸ Briefly, the 1,2-DHN sample (Aldrich, 99+% purity) was sublimed from a small quartz tube located in close proximity to the deposition window. The sublimed sample was codeposited with argon gas onto a 12 K CsI window cooled by a closed-cycle helium cryostat (APD Displex). After 2–3 h of deposition, infrared absorption spectra were collected using a NICOLET Magna 560 FT-IR spectrometer (0.5 cm^{-1} resolution). Annealing of the matrix (heating to 35 K and recooling to 12 K), as well as photolysis with a medium-pressure 100 W Hg lamp, were also performed to induce secondary reactions.

IR Action Spectroscopy. The experiments on the gaseous protonated species were carried out with a 4.7 T Fourier-transform ion cyclotron resonance mass spectrometer (FTICR-MS), coupled to a free electron laser with a tunable output in the infrared.²⁹ Trapped ions are exposed to 5 μs long laser macropulses (100 mJ, 10 Hz). Each macropulse contains a group of 0.3–0.5 ps fwhm pulses separated by 1 ns. The experimental apparatus has been previously described.³⁰ The protonated sample was formed by electrospray ionization of a 80:20:0.02 methanol/water/acetic acid solution of 5 mM 1,2-DHN with an infusion rate of 30 $\mu\text{L}/\text{min}$. Protonation presumably occurs in the electrospray source with protons provided by the solvent species. Two IRMPD channels were observed from the protonated 1,2-DHN (m/z 131): m/z 129 and 91. The IRMPD spectrum was determined by the decrease in the parent m/z 131 peak and the increase of the m/z 129 and 91 peaks, as a function of the IR laser frequency. The infrared bands observed by monitoring the m/z 129 channel were approximately twice as intense as the m/z 91 bands.

Computational Methods

All calculations were carried out using the Gaussian 03 suite of programs.³¹ The equilibrium geometries, harmonic vibrational frequencies, and dissociation energies were calculated using the B3LYP functional^{32,33} with a 6-31++G(d,p) basis set. The potential energy surface (PES) for selected dissociation reactions were calculated with a 6-31G(d,p) basis set. The transition states connecting the stable minima were investigated via the QST2 or QST3 searching procedures incorporated in Gaussian 03.³¹ The electronic energies were corrected for zero point vibrational energies without scaling.

Results and Discussion

A. Infrared Spectra. 1. Absorption Spectrum of Neutral 1,2-DHN. Although our main goal was the study of the protonated 1,2-DHN cation via IRMPD spectroscopy and the use of density functional calculations to determine the site of protonation and the most probable dissociation pathways, the reliability of this theoretical approach was checked by comparing the experimental and theoretical IR absorption spectra of neutral 1,2-DHN. It

- (19) Banisaukas, J.; Szczepanski, J.; Eyler, J.; Vala, M.; Hirata, S.; Head-Gordon, M.; Oomens, J.; Meijer, G.; von Helden, G. *J. Phys. Chem. A* **2003**, *107*, 782–793.
- (20) Beegle, L. W.; Wdowiak, T.; Harrison, J. G. *Spec. Acta A* **2001**, *57*, 737–744.
- (21) Lorenz, U. J.; Solca, N.; Lemaire, J.; Maitre, P.; Dopfer, O. *Angew. Chem., Int. Ed.* **2007**, *46*, 6714–6716.
- (22) Duley, W. W.; Williams, D. A. *Interstellar Chemistry*; Academic Press: New York, 1984.
- (23) Herbst, E. *Annu. Rev. Phys. Chem.* **1995**, *46*, 27–54.
- (24) Glover, S. C. O. *Astrophys. J.* **2003**, *584*, 331–338.
- (25) Kleinhaus, H.; Wijting, R. L. C.; Havinga, E. *Tetrahedron Lett.* **1971**, *12*, 255–258.
- (26) Duguid, R. J.; Morrison, H. *J. Am. Chem. Soc.* **1991**, *113*, 1271–1281, and references therein.
- (27) Tomasello, G.; Ogliao, F.; Bearpark, M. J.; Robb, M. A.; Garavelli, M. *J. Phys. Chem. A* **2008**, *112*, 10096–10107.

- (28) Szczepanski, J.; Roser, D.; Personette, W.; Eyring, M.; Pellow, R.; Vala, M. *J. Phys. Chem.* **1992**, *96*, 7876–7881.
- (29) Oepts, D.; van der Meer, A. F. G.; van Amersfoort, P. W. *Infrared Phys. Technol.* **1995**, *36*, 297–308.
- (30) Valle, J. J.; Eyler, J. R.; Oomens, J.; Moore, D. T.; van der Meer, A. F. G.; von Helden, G.; Meijer, G.; Hendrickson, C. L.; Marshall, A. G.; Blakney, G. T. *Rev. Sci. Instrum.* **2005**, *76*, 023103.
- (31) Frisch, M. J. *Gaussian 03, Revision B.05*; Gaussian, Inc.: Wallingford CT, 2003.
- (32) Becke, A. D. *J. Chem. Phys.* **1993**, *98*, 5648–5652.
- (33) Lee, C.; Yang, W.; Parr, R. *Phys. Rev. B* **1998**, *37*, 785–789.

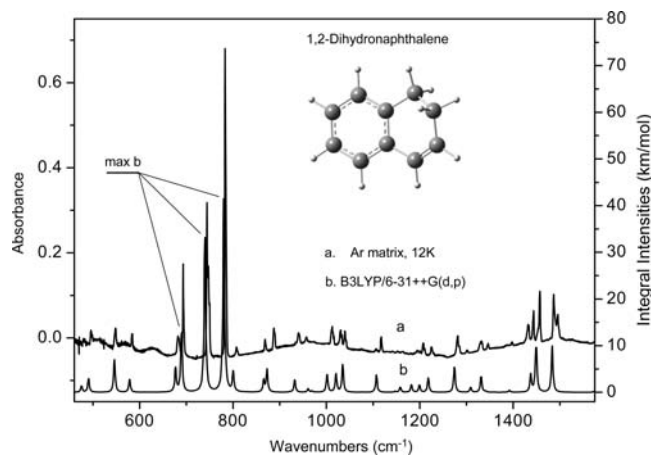


Figure 1. Infrared absorption spectrum of neutral 1,2-DHN in solid argon at 12 K. Upper panel, experimental spectrum; lower panel, calculated spectrum. Band assignments are listed in Table 1.

was also of interest to determine the effect on the IR spectrum of naphthalene by addition of two hydrogens in 1,2-DHN.

The observed infrared absorption spectrum of neutral 1,2-DHN in an Ar matrix (12 K) is given in the upper panel of Figure 1 and the calculated spectrum in the lower panel. The band positions and intensities of both spectra, along with their proposed mode assignments, are listed in Table 1.

There are three major differences between the 1,2-DHN and naphthalene^{28,34} spectra. First, 1,2-DHN possesses two extra, relatively strong bands, at 744.2 and 693.3 cm^{-1} (see Figure 1 and Table 1). Both bands are assigned to CCH out-of-plane vibrations. Second, the predicted 1437.9, 1447.7, and 1449.6 cm^{-1} modes are predominantly $\text{HC}(\text{sp}^3)\text{H}'$ scissor vibrations. The 1432.4, 1444.0, and 1457.5 cm^{-1} experimental bands assigned to these modes match reasonably well (Table 1). The third difference is that there are four extra, relatively strong bands in the 2840–2950 cm^{-1} region, all ascribed to $\text{C}(\text{sp}^3)\text{H}$ stretching modes (Table 1). In Ar matrices, naphthalene displays only one strong band, a CCH out-of-plane mode at 783 cm^{-1} , moderately intense CH stretching bands in the 3030–3080 cm^{-1} region, and relatively weak bands in all other regions.^{28,34,35}

As can be seen from Figure 1 and Table 1, the experimental and predicted band energies and relative intensities for 1,2-DHN are in quite good agreement in both the mid-IR and CH stretch regions. We conclude that the IR spectrum of 1,2-DHN, which contains aliphatic and aromatic carbons with attached hydrogens, can be well described by B3LYP/6-31++G(d,p) calculations and that this theory can be applied with confidence to the trihydronaphthalene cation (THN^+). Both are closed-shell systems. A recent paper by Ricca and Bauschlicher on the catalytic formation of H_2 by CH_3^+ supports this level of theory for the present type calculations.³⁶

2. Action Spectrum of Protonated 1,2-DHN. The infrared action spectrum of vapor phase protonated 1,2-DHN is shown in Figure 2, with band positions and proposed assignments given in Table 2.

The lowest energy IRMPD band observed at 780 cm^{-1} and a shoulder at 762 cm^{-1} correspond well with the computed CC/CH out-of-plane modes at 777.7 and 756.6 cm^{-1} (marked a and

b in Figure 2). Calculations predict relatively weak CC/CH in-plane modes in the 1120–1330 cm^{-1} range (marked f–l). As some of the bands in this region overlap, their assignment should be considered tentative.

The IRMPD spectrum reveals a large enhancement in fragment yield in the 1370–1470 cm^{-1} range. This part of the spectrum is assigned to five HCH scissor modes involving the sp^3 carbons (marked m, n, o, p, and r in Figure 2). These modes couple weakly with the CH in-plane bending vibrations (Figure 3). Since the scissor modes exhibit large displacements from equilibrium, they are expected to have relatively large anharmonicities. To test this, the anharmonic vibrational spectrum for protonated 1,2-DHN was calculated at the B3LYP/6-31G(d,p) level and compared to the analogous harmonic spectrum. The difference in calculated mode frequencies, $\omega(\text{harmonic}) - \nu(\text{anharmonic})$, is an indicator of mode anharmonicity. For modes with a high anharmonicity (e.g., CH stretch modes) the differences are in the range 122–146 cm^{-1} , with the highest value belonging to the $\text{C}(\text{sp}^3)\text{H}$ stretch. For the 600–1650 cm^{-1} fingerprint region, the $\omega(\text{harmonic}) - \nu(\text{anharmonic})$ differences lie between 10–47 cm^{-1} , with the $\text{HC}(\text{sp}^3)\text{H}$ scissor modes showing the highest anharmonicity and the CH out-of-plane modes, the lowest.

Mode coupling, as reflected by anharmonicity, can influence the lifetime of intramolecular vibrational energy redistribution (IVR), which for gas phase protonated 1,2-DHN is expected to be in the sub-picosecond range.³⁷ Vibrational anharmonicity also influences the intensity of the IRMPD bands observed.^{38,39} In the coronene cation, the 777 cm^{-1} IR-active CC/CH out-of-plane mode was not observed in IRMPD because its predicted maximum internal energy was lower than the dissociation limit.⁴⁰ This may also be the case here for the four relatively weak CC/CH out-of-plane modes predicted at 695.4, 905.4 (c), 985.7 (d), and 1059.8 cm^{-1} (e), all silent in the IRMPD spectrum, see Figure 2. The strong IRMPD band at 1588 cm^{-1} is assigned primarily to the CC stretch, predicted at 1613.3 cm^{-1} , with a large intensity of 307 km/mol . The 1588 cm^{-1} (6.3 μm) band is in reasonable agreement with the strong 1599 cm^{-1} (6.25 μm) band reported for protonated naphthalene by the Dopfer group²¹ and the 1607 cm^{-1} (6.22 μm) band in protonated benzene by the Duncan group.⁴¹ Calculations by the Allamandola group on many protonated PAHs predict a very strong mode in the 1590 (6.29)–1580 cm^{-1} (6.33 μm) range which coincides approximately with the 6.2 μm UIR emission band observed from space.³⁹ However, the calculated and experimental bands for protonated species, including the 1588 cm^{-1} band observed here for protonated 1,2-DHN, are in better agreement with the 1590 cm^{-1} (6.29 μm) UIR emission feature which was resolved in higher resolution spectra obtained from the ISO satellite.⁴²

The aromatic CH stretching modes in protonated 1,2-DHN have very low predicted integral intensities (below 5 km/mol),

(34) Hudgins, D. M.; Sandford, S. A.; Allamandola, L. J. *J. Phys. Chem.* **1994**, *98*, 4243–4253.

(35) Szczepanski, J.; Vala, M. *Astrophys. J.* **1993**, *414*, 646–655.

(36) Ricca, A.; Bauschlicher, C. *Chem. Phys. Lett.* **2003**, *463*, 327–329.

(37) Boyall, D.; Reid, K. L. *Chem. Soc. Rev.* **1997**, *26*, 223–232.

(38) Oomens, J.; van Roij, A. J. A.; Meijer, G.; von Helden, G. *Astrophys. J.* **2000**, *542*, 404–410.

(39) Oomens, J.; Tielens, A. G. G. M.; Sartakov, B. G.; von Helden, G.; Meijer, G. *Astroph. J.* **2003**, *591*, 968–985.

(40) Hudgins, D. M.; Bauschlicher, C. W., Jr.; Allamandola, L. J. *Spectro. Acta A* **2001**, *57*, 907–930.

(41) Douberly, G. E.; Ricks, A. M.; Schleyer, P. V. R.; Duncan, M. A. *J. Phys. Chem. A* **2008**, *112*, 4869–4874.

(42) Peeters, E.; Hony, S.; Van Kerckhoven, C.; Tielens, A. G. G. M.; Allamandola, L. J.; Hudgins, D. M.; Bauschlicher, C. W. *Astron. Astrophys.* **2002**, *390*, 1089–1113.

Table 1. Calculated and Experimental IR Absorption Spectra of 1,2-DHN with Proposed Band Assignments

mode ^a	$\nu_{\text{cal}}^b/\text{cm}^{-1}$	$\nu_{\text{exp}}^c/\text{cm}^{-1}$	mode ^a	$\nu_{\text{cal}}^b/\text{cm}^{-1}$	$\nu_{\text{exp}}^c/\text{cm}^{-1}$
$\varepsilon+\tau$	260.5 (0.09)		$\alpha+\beta$	1158.3 (0.02)	1155.3 (0.01)
$\varepsilon+\tau$	382.2 (0.02)		$\alpha+\beta$	1182.2 (0.04)	1195.0 (0.01)
$\varepsilon+\tau$	413.8 (0.07)	416.1 (0.05)	$\alpha+\beta$	1199.4 (0.04)	1207.3 (0.04)
$\varepsilon+\tau$	475.5 (0.03)	479.7 (0.02)	$\alpha+\beta$	1218.3 (0.07)	1225.1 (0.03)
$\varepsilon+\tau$	490.6 (0.07)	495.7 (0.04)	$\alpha+\beta$	1274.3 (0.13)	1281.6 (0.08)
$\varepsilon+\tau$	546.0 (0.16)	548.3 (0.09)	$\alpha+\beta+\text{R}$	1309.1 (0.02)	1301.5 (0.01)
$\varepsilon+\tau$	578.6 (0.06)	584.0 (0.04)	$\alpha+\beta+\text{R}$	1331.6 (0.08)	1332.7 (0.06)
$\alpha+\beta$	677.0 (0.12)	682.3 (0.09)	$\pi+\varepsilon+\text{R}$	1437.9 (0.09)	1432.4 (0.07)
$\varepsilon+\tau$	689.7 (0.30)	693.3 (0.25)	$\pi+\varepsilon+\text{R}$	1447.7 (0.05)	1444.0 (0.09)
$\alpha+\beta$	740.0 (0.77)	744.2 (0.82)	$\pi+\varepsilon+\text{R}$	1449.6 (0.21)	1457.5 (0.16)
$\varepsilon+\tau$	780.4 (1.0)	783.1 (1.0)	$\text{R}+\varepsilon$	1483.8 (0.23)	1487.0 (0.14) 1495.9 (0.08) ^d
$\varepsilon+\tau$	800.4 (0.10)	807.6 (0.04)	$\text{r}(\text{C}(\text{sp}_3)\text{H})$	2852.4 (0.60)	2842.1 (0.28) 2846.5 (0.25) ^d
$\varepsilon+\tau$	865.9 (0.06)	868.9 (0.05)	$\text{r}(\text{C}(\text{sp}_3)\text{H})$	2866.0 (0.93)	2898.4 (0.63) 2909.3 (0.13) ^d
$\alpha+\beta$	872.9 (0.11)	887.6 (0.08)	$\text{r}(\text{C}(\text{sp}_3)\text{H})$	2932.6 (0.86)	2946.1 (0.64)
$\varepsilon+\tau$	932.3 (0.06)	940.4 (0.05)	$\text{r}(\text{C}(\text{sp}_3)\text{H})$	2938.8 (0.67)	2952.7 (0.45)
$\varepsilon+\tau$	960.9 (0.02)	957.1 (0.02)	R	3021.0 (0.07)	3022.5 (~0.1)
$\text{R}+\beta$	1001.6 (0.09)	1012.8 (0.08)	R	3025.7 (0.30)	3026.5 (0.38)
$\text{R}+\beta$	1020.7 (0.09)	1030.8 (0.07)	R	3042.5 (0.63)	3044.6 (0.55) 3067.9 (0.17) ^d
$\beta+\text{R}$	1035.0 (0.14)	1039.6 (0.07)	R	3044.3 (0.79)	
$\beta+\text{R}$	1107.1 (0.09)	1117.6 (0.06)	R	3059.6 (0.56)	3077.3 (0.24) 3102.8 (0.07) ^d

^a Notation used: ε and τ are CCC and CCH out-of-plane vibrations, α and β are CCC and CCH in-plane bending, π are $\text{HC}(\text{sp}^3)\text{H}$ scissors, while R and r are CC and CH stretching modes, respectively. ^b Vibrational frequencies of calculated (B3LYP/6-31++G(d,p)) spectrum are scaled uniformly by scaling factors of 0.975 and 0.955 for mid-IR and CH stretching modes, respectively. The integral intensity for the 780.4 cm^{-1} strongest band is 43 km/mol . Modes with relative intensities (in parentheses) larger or equal to 0.02 are listed only. ^c Ar matrix experiment at 12 K, this work. ^d Trapped in a secondary matrix site.

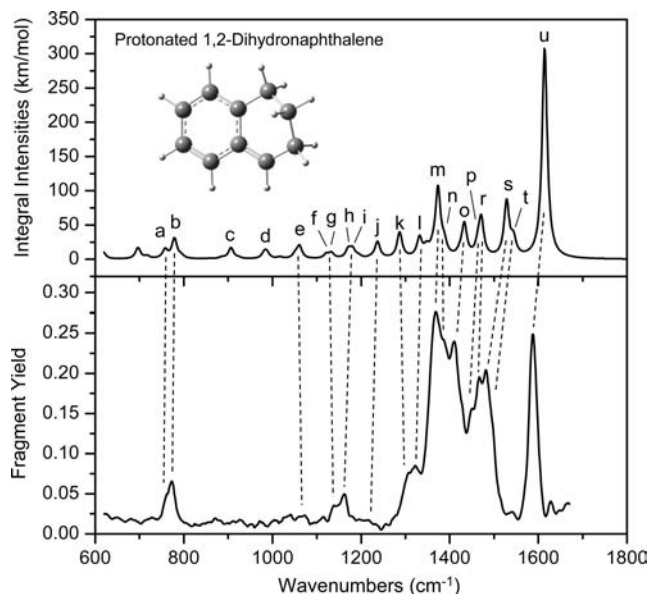


Figure 2. Infrared multiple photon dissociation spectrum of vapor phase protonated 1,2-DHN (lower panel) and its calculated infrared spectrum (upper panel). Band assignments are listed in Table 2.

as is typical for a wide range of PAH cations. However, the aliphatic $\text{C}(\text{sp}^3)\text{H}$ stretching modes, while shifted to lower energies, do have higher integral intensities, as can be seen in Table 2.

B. Formation of Trihydronaphthalene Cation (THN^+). There are two possible reactions leading to the formation of THN^+ from 1,2-DHN.



The first is the protonation of the neutral parent, while the second is the hydrogenation of the parent cation. Reaction energies for

these two reactions, calculated with the B3LYP/6-31++G(d,p) functional/basis set, give -6.11 eV for the first and -2.94 eV for the second reaction. Ricca et al.¹⁷ recently reported a value of -3.01 eV (-69.4 kcal/mol) for the energy for the second reaction calculated at the B3LYP/6-31G(d) level. While both reactions are exothermic, only the first is expected to produce the THN^+ parent (m/z 131) in our electrospray/mass spectrometry experiment. However, as Hirama et al. point out, either reaction could occur with various PAHs in interstellar space, provided the constituent reactants are present in sufficient quantity.⁹

C. Protonation Site. The preferred protonation site on 1,2-DHN was investigated by calculating the relative stabilities of all the possible isomers formed by protonation at sites 3–8. The zero-point-corrected results are listed in Table 3. The most stable isomer is the 1,2,3- THN^+ cation, followed by 1,2,7- THN^+ ($+0.34$ eV) and 1,2,5- THN^+ ($+0.43$ eV). The least stable species, 1,2,4- THN^+ , is more than 1 eV higher in energy. These results mimic calculations reported by Ricca et al.¹⁷ Also shown in Table 3 are the proton affinities for neutral 1,2-DHN which can be seen to parallel the relative stabilities of the cationic THN species. Stabilities of the neutral species 1,2,X-THN ($X = 3-8$) are also included in the table. Thus, both stability and proton affinity calculations point to 1,2,3- THN^+ as the species responsible for the observed IRMPD spectrum. Further support for this conclusion comes from the calculated IR spectrum of 1,2,7- THN^+ which predicts two strong bands in the 1600 cm^{-1} region where only one is observed.

D. Dissociation Channels. When protonated 1,2-DHN is irradiated by multiple infrared photons it dissociates along two different channels, one yielding an ionic fragment with m/z 129 and the other a fragment with m/z 91. To investigate possible pathways to these products and their energy requirements, a series of calculations of the relevant potential energy surfaces (PESs) were performed. Each is discussed in turn below.

1. m/z 129 Fragmentation Channel. In this channel, the m/z 131 parent loses two mass units. It is significant that only two mass units are lost and not one, three, or higher integral

Table 2. Calculated Vibrational Absorption and Experimental IR Spectra of Protonated 1,2-DHN with Proposed Band Assignments

mode ^{a,b}	$\nu_{\text{cal}}/\text{cm}^{-1}$	$\nu_{\text{exp}}/\text{cm}^{-1}$	mode ^{a,b}	$\nu_{\text{cal}}/\text{cm}^{-1}$	$\nu_{\text{exp}}/\text{cm}^{-1}$
$\varepsilon+\tau$	615.5 (0.04)		(k) $R+\beta+\tau$	1286.1 (0.12)	1308
$\varepsilon+\tau$	695.4 (0.05)		(l) $R+\alpha+\beta$	1330.8 (0.09)	1322
(a) $\varepsilon+\tau$	756.6 (0.04)	762 sh	$R+\alpha+\beta$	1346.8 (0.04)	
(b) $\varepsilon+\tau$	777.7 (0.10)	780	$R+\alpha+\beta$	1360.6 (0.03)	
(c) $\varepsilon+\tau$	905.4 (0.05)		(m) π	1372.5 (0.32)	1368
$\varepsilon+\tau$	980.0 (0.02)		(n) $\pi+\beta$	1386.5 (0.06)	1386 sh
(d) $\varepsilon+\tau+R$	985.7 (0.03)		(o) $\pi+\beta$	1431.9 (0.15)	1411
$\alpha+\beta$	1050.6 (0.02)		(p) $\pi+\beta$	1463.2 (0.05)	1452 sh
(e) $\varepsilon+\tau+R$	1059.8 (0.05)		(r) $\pi+\beta$	1470.3 (0.17)	1467
(f) $\alpha+\beta$	1120.5 (0.02)	1139	(s) $R+\beta$	1527.4 (0.26)	1482
(g) $\varepsilon+\tau+\beta$	1132.1 (0.03)		(t) $R+\beta$	1542.9 (0.08)	1500 sh
(h) $\alpha+\beta$	1170.2 (0.04)	1169	(u) $R+\beta$	1613.3 (1.00)	1588
(i) $\beta+R$	1179.8 (0.04)		r(C(sp ³)H)	2813.8 (0.10)	
(j) $\beta+R+\tau$	1236.0 (0.08)	~1233	r(C(sp ³)H)	2923.3 (0.04)	

^a Notation used: ε and τ are CCC and CCH out-of-plane, α and β are CCC and CCH in-plane bending, π are HC(sp³)H scissors, while R and r are CC and CH stretching modes, respectively. ^b The frequencies marked by the letters (a)–(u) refer to bands displayed in Figure 2. ^c Vibrational frequencies of calculated (B3LYP/6-31++G(d,p)) spectrum are scaled uniformly by scaling factors of 0.975 and 0.955 for mid-IR and C–H stretching modes, respectively. The integral intensity for the 1613.3 cm⁻¹ band is 307 km/mol. Only those modes with relative intensities (in parentheses) are equal to or greater than 0.02 are listed. ^d IR multiphoton photodissociation experiment, this work.

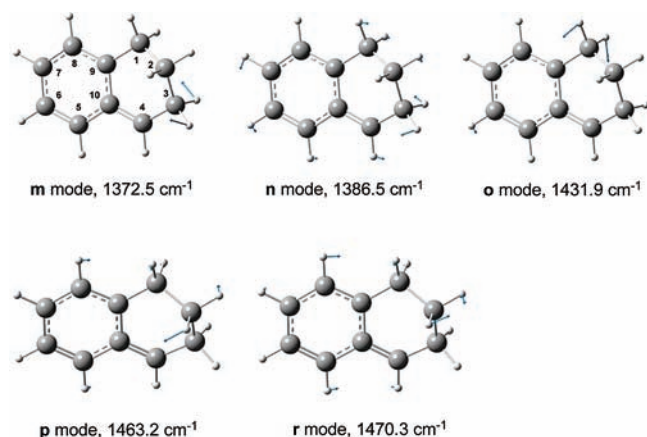


Figure 3. Vibrational modes of protonated 1,2-DHN in the 1370–1470 cm⁻¹ energy range. All are mostly $HnCnHn'$ ($n = 1, 2, 3$) scissor modes involving the three sp³ carbon atoms, C1, C2, and C3. For these modes a large resonance enhancement in the experimental IRMPD spectrum is observed (see Figure 2). The atomic displacements from equilibrium are shown by arrows.

Table 3. Calculated (B3LYP/6-31+G(d,p)) Relative Ground State Total Energies of Cationic and Neutral 1,2,*X*-THN ($X = 3$ –8) and Proton Affinities of Neutral 1,2-DHN

<i>X</i>	cation $\Delta E_{\text{rel}}/\text{eV}$	neutral $\Delta E_{\text{rel}}/\text{eV}$	proton affinities/eV
3	0.0	0.0	6.11
4	1.07	1.54	5.04
5	0.43	0.79	5.67
6	0.62	0.92	5.49
7	0.34	0.71	5.77
8	0.70	0.93	5.42

multiples. If any of the latter were observed, one would conclude that individual hydrogen atoms were being stripped from the parent, but with only two mass units ejected, we argue that this represents the ejection of the hydrogen molecule. We assume that the hydrogens which form H₂ come from those atoms already attached to the PAH framework and not, as others have suggested, from one hydrogen attached to the framework and another incoming, free-flying hydrogen atom. Because of their proximity to each other, we consider the hydrogens attached to the aliphatic sp³ carbons as the most probable to form H₂. There are three sets of aliphatic hydrogen pairs on THN⁺ to consider, on carbons 1, 2, and 3. Certain vibrational motions, the scissor-

like HCH modes, parallel the reaction pathway necessary to form molecular hydrogen. Figure 3 shows the scissor modes on the three carbons. The 1431.9 cm⁻¹ mode is predominantly on C1, the 1463.2 and 1470.3 cm⁻¹ modes on C2, and the 1372.5 and 1386.5 cm⁻¹ modes on C3. It is expected that the amplitudes of these modes will become very large and their displacements range far from equilibrium. One could envisage that as the two H atoms approach each other in a large amplitude motion, H–H' bond formation will be initiated and, simultaneously, the CH and CH' bond lengths will lengthen. The culmination of this process would result in the formation of the H₂ molecule and its subsequent ejection from the parent.

This scenario was explored theoretically by calculating, at the B3LYP/6-31G(d,p) level, the singlet PES for this process on the three different aliphatic carbon sites. The results are shown in Figure 4a–c and discussed below.

The first reaction considered involved the hydrogens attached to carbon C1 (see Figure 4a). The calculation was performed by searching via a full geometry optimization for a complex between H₂ and the fragment **B** shown in Figure 4a. This stable complex lies 3.759 eV above the THN⁺ parent. A transition state search to the product from the parent **A** was next performed using the QST2 routine from Gaussian 03. A transition state **TS1**, located 3.843 eV above the parent cation, was found and in it both CH bond lengths have increased, from 1.09 to 2.304 and 1.804 Å. The H–H bond length has also decreased, almost to the molecular length of 0.7428 Å. **TS1** is only lightly above (0.084 eV) the stable, but weakly bound complex **B**. With a further stabilization of 0.02 eV, H₂ is ejected from the parent and the stable fragment **C** formed. Increasing the distance between H₂ and fragment **C** does not change the energy of the system much, so it was impossible to locate any transition state between **B** and **C**. This almost flat PES is indicated in Figure 4a by a dashed line. In both **B** and **C** the C2–C3 bond has opened up, to 1.644 and 1.650 Å, respectively. Although **C** is a stable fragment, one might expect that one of the hydrogens on C2 will migrate to the “naked” carbon C1. This was investigated by determining the energy required to form the bridge structure by scanning the bond angle C1–C2–H₂. An energy maximum was found with a structure similar to the transition state **TS2**. The actual transition state, **TS2**, in which a hydrogen bridges C1 and C2 was found with a calculated energy barrier of only 0.618 eV. This transition state connects

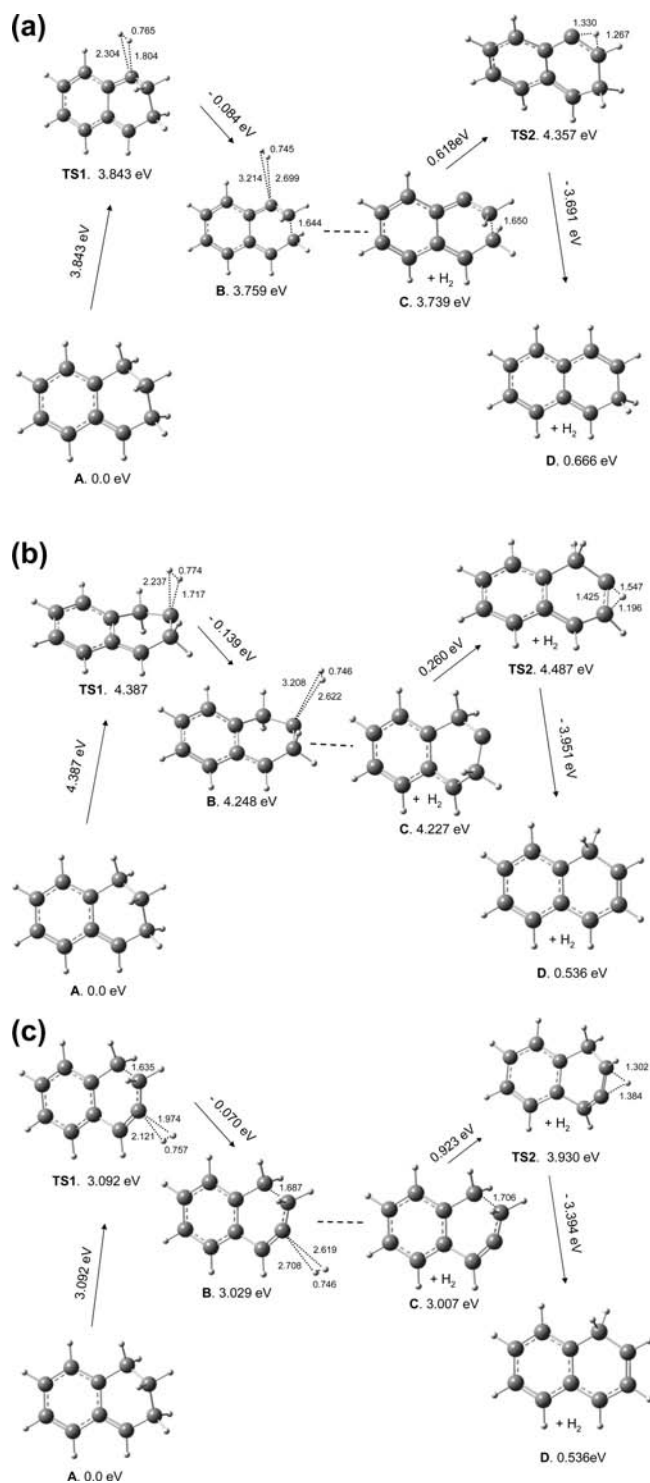


Figure 4. Calculated PES (B3LYP/6-31G(d,p)) for the H₂ abstraction reaction from the (a) C1 carbon, (b) C2 carbon, and (c) C3 carbon in protonated 1,2-DHN. Relative electronic energies (ZPE corrected) in eV are indicated.

C with the 3-hydronaphthalene cation (D). While the final product D lies only 0.666 eV above the initial reactant A, the actual reaction pathway requires substantially greater energy, but this energy can be provided by either 15–25 mid-infrared photons or a single near-UV photon. Such H atom migrations about an aromatic ring in the naphthalene radical cation (“methathesis” channel) have previously been found by Jolibois

et al. who showed that they were of lower energy than either the H atom or H₂ molecule dissociation channels.¹⁶

The second reaction considered was the removal of H₂ from the C2 (sp³) site. Four stable structures (A–D) plus two transition states (TS1 and TS2) were again found (Figure 4b). TS1, which connects reactant A with the stable, weakly bound complex B, is located 4.387 eV above A, and exhibits one imaginary vibrational frequency (−375.6 cm^{−1}). This mode is a composite C–H₂ stretch and H–H stretch in which the C2–(H2H2′) bond lengthens and the H2–H2′ bond shortens. The H₂-dissociated system C has a marginally lower energy (0.021 eV) than B. The bare carbon C2 can acquire a hydrogen from the neighboring carbon by climbing a small 0.26 eV barrier to TS2. This reaction terminates at D, the stable 1-HN (1-hydronaphthalene) cation. One imaginary frequency (−893 cm^{−1}) was found for TS2 indicating a movement of H3′ in a direction almost parallel to the C2C3 bond. In sum, the dissociation of H₂ from the C2(sp³) site of protonated 1,2-DHN requires 4.387 eV energy and an additional 0.26 eV energy to form the lowest energy singly protonated naphthalene isomer, 1-hydronaphthalene cation (*m/z* 129).

The third reaction considered was the ejection of H₂ from the C3 (sp³) site. The calculated PES for this reaction is displayed in Figure 4c. The first transition state TS1 lies 3.092 eV above reactant A. All the energetically excited structures (TS1, B, C) have a partially opened C1–C2 bond, with the largest one (1.706 Å) occurring in C. Transition state TS2 lies 0.923 eV above C and connects C with the 1-hydronaphthalene cation product. Our initial attempts to find the transition state TS2 for this and the C1 site reaction (Figure 4a) were unsuccessful. To circumvent this problem we calculated the energy profile by stepping the H2C2C3 bond angle by 1° increments (and analogously H2C2C1 in Figure 4a) while fully optimizing all other degrees of freedom. This allowed us to find the approximate structure for TS2, which was then used in the QST3 transition state search procedure. Once over the TS2 barrier the reaction proceeds steeply downhill and finishes with the products D, 1-hydronaphthalene cation, and H₂ (and, in Figure 4a, 3-hydronaphthalene cation and H₂).

In summary, the reaction energy barriers which must be overcome to eject H₂ from THN⁺ are 3.843 (H₂ removal from C1), 4.387 (H₂ removal from C2), and 3.092 eV (H₂ removal from C3). Additional energies of 0.618, 0.260, and 0.923 eV are required to form the 3-hydronaphthalene cation (Figure 4a reaction) or 1-hydronaphthalene cation (Figure 4b and c reactions), respectively.

To provide further insight into the mechanism of H₂ formation, the IRMPD experiment was rerun using deuterated solvents exclusively (i.e., D₂O, CH₃OD, and CH₃COOD). If a solvent deuteron combines with neutral 1,2-DHN, an ionic species with *m/z* 132 is formed. If the deuteron combines with the hydrogen on C3 as HD and dissociates from the 1,2-dihydro-3-deuteronaphthalene cation, the mass of the remaining ionic fragment would be *m/z* 129, and this would prove that the mechanism of dissociation involves only the C3 carbon. On the other hand, if the exiting molecular hydrogen is H₂ (with a remaining ionic fragment of mass *m/z* 130), it can be argued that the hydrogens from C1 and/or C2 were involved. It is of course impossible to distinguish between dissociation from the C1 or C2 carbons.

The experiment showed that a strong peak at *m/z* 132 was observed which, upon absorption of multiple infrared photons, fragmented to *m/z* 130 and 129 ions (as well as *m/z* 91 and 92 ions). Though the spectral scan was noisy, the *m/z* 129 and 130

ions channels were approximately equal in intensity. Thus, we conclude that both hydrogens on C1 (and/or C2) and the hydrogen and deuterium on C3 are involved in the formation of the exiting molecular hydrogen species.

2. m/z 91 Fragment. In the second dissociation channel, the m/z 131 parent dissociates to a m/z 91 species, equivalent to $C_7H_7^+$, and a neutral species C_3H_4 . The m/z 131 parent dissociates along two channels yielding m/z 129 and m/z 91 products in approximately a 2:1 ratio.

Parts of the potential energy surface of the 1,2,3-THN⁺ species were calculated to determine the most probable dissociation pathways and estimated energy barriers leading to a m/z 91 product. The lengths of three aliphatic C–H bonds were incremented to a total elongation ($\Delta r(\text{C–H})$) of 3.0 Å. At each step the geometry was optimized (except for the C–H bond length) and the total energy determined. Interestingly, the results differ substantially depending on which C–H bond is stretched. This no doubt reflects the nonplanarity of this ring and the fact that the immediate surroundings of the hydrogens attached to the aliphatic carbons are different. For example, if the C3–H3 bond is stretched, the H3 hydrogen migrates to C4, forming the 1,2,4-THN cation. However, if the C3–H3' bond is stretched, the H3' hydrogen exchanges with H4. Stretching either the C2–H2 or the C2–H2' bond results in a different reaction pathway altogether. Because C2 and its attached hydrogens, H2 and H2', are bracketed on both sides by hydrogen-bearing aliphatic carbons, steep repulsive potentials exist and exert an influence as H2 (or H2') is stretched. For example, as C2–H2 is stretched to $\Delta r(\text{C2–H2}) = 2.1$ Å, the energy increases to 5.6 eV, but, with additional stretching, the H2 atom hops to the C9 carbon. This unexpected jump to a carbon shared by both rings, and the hydrogen migrations discussed above, demonstrate clearly how difficult it is to eject a single H atom from 1,2,3-THN⁺. If displaced from their equilibrium positions, single hydrogen atoms in THN⁺ apparently prefer to change positions on the carbon frame than to actually escape from its force field. Below we discuss the energetics of forming the m/z 91 ion fragment.

Stretching the C3–H3 bond in 1,2,3-THN⁺ by 0.5 Å, requires ca. 1.28 eV, but at this energy the H3 hydrogen hops to C4 and forms the 1,2,4-THN⁺ isomer (C, Figure 5). During this process the C1–C2 bond length increases slightly from 1.534 to 1.539 Å, with other single bonds remaining smaller: $r(\text{C9–C1}) = 1.516$, $r(\text{C2–C3}) = 1.499$, and $r(\text{C4–C10}) = 1.498$ Å. Since it is now the longest in the ion, it is likely that the C1–C2 bond will rupture first. A modest 0.57 eV energy input lengthens it to ca. 2.5 Å, an essentially broken bond. Scanning the C4–C10 bond length shows that with an input of 1.90 eV, the H4' atom first bridges the C4 and C10 carbons (structure E) and finally migrates to C10, yielding structure F, together with a 1.11 eV release of energy. C10 is now aliphatic with 4 single bonds. Of these, the C10–C4 bond is long (1.540 Å) and may be ruptured with an additional 2.61 eV energy. The $C_7H_7^+$ fragment is now separated from C_3H_4 .

These results are consistent with the products seen in the deuterated solvent experiment. Recall that ionic products of m/z 91 values 91 and 92 were observed upon infrared multiple photon dissociation of the m/z 132 parent ion. If, as proposed here, the deuterium is added at position 3 and then migrates to position 4, the bridge structure (E) may have either a deuterium or a hydrogen atom bridging carbons 4 and 10. This would then lead to the final ionic product (G) with a hydrogen in the ortho

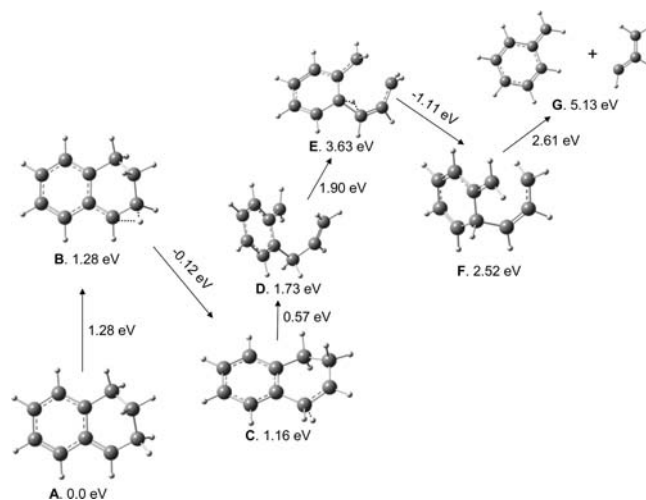


Figure 5. Calculated PES (B3LYP/6-31G d,p) for various bond ruptures (or hydrogen migration) reactions in protonated 1,2-DHN. At each bond length (or HCC angle) increment all other degrees of freedom were fully optimized. Relative electronic total energies (not ZPE corrected) in eV are indicated.

position (with m/z 91, i.e., $C_7H_7^+$) or a deuterium (with m/z 92, i.e., $C_7DH_6^+$).

In summary, by lengthening the C3–H3 bond, we found that 1,2,3-THN⁺ converts to 1,2,4-THN⁺ (with 1.28 eV input). With an additional 0.57 eV, the C1–C2 bond breaks. Stretching the C4–C10 bond results in H4' first bridging these carbons and finally migrating fully to C10. Further stretching of C4–C10 results in it breaking. The net energy input necessary to produce the observed m/z 91 product is 5.13 eV and, interestingly, involves two hydrogen migrations. The proposed mechanism has the advantage that the four separate steps require small energy inputs, from 0.57 to 2.61 eV. Whether delivered by multiple infrared photons or single separate visible photons, if the produced fragments retain any excess energy, it is likely that they will further isomerize to the known stable products, monocyclic tropylium ion, $C_7H_7^+$ (m/z 91), and propyne, $CH_3C\equiv CH$.

E. H₂ Formation in the Interstellar Medium. Although it has long been acknowledged that H₂ is formed in the interstellar medium by H atom combination on small dust grains, it has recently been proposed that PAHs may act as catalytic centers for the formation of H₂. Independently, Bauschlicher⁸ and Hirami et al.⁹ suggested a H₂ formation model which involves the capture of a hydrogen atom by a PAH cation, followed by the abstraction of the added hydrogen by another incoming H atom, to form H₂. This model is an attractive one since the first H addition reaction is exothermic and the second abstraction reaction has a zero or very small activation barrier, enabling the overall reaction to occur at low temperatures. The primary disadvantage is the stringent geometric constraint on the incoming second H atom. It appears that it would need to approach the singly hydrogenated PAH in the vicinity of the original hydrogenation site in order to form the complex required prior to H₂ formation and ejection.

The present model differs from the former in that the H₂ molecule ejected originates from the two hydrogens attached to an aliphatic carbon in the PAH framework. This obviously requires energy input and is envisaged to occur by the absorption of a ultraviolet (UV) photon followed by internal conversion to high-lying vibration levels of the ground electronic state. Large amplitude vibrations of the aliphatic carbons' HCH

scissors modes are proposed to lead to the formation of H₂. The required energies are in the 3–4 eV range. As Ricca et al.¹⁷ have shown theoretically, sequential hydrogenation preferentially occurs on adjacent carbons on one ring. If a PAH has two or more adjacent aliphatic carbons, hydrogens adjacent to the H₂ ejection site will bridge and finally migrate to that site after ejection, thereby enhancing the aromaticity and stability of the PAH ring. Hydrogen migration appears to occur about the ring with relative ease, so any geometry constraint on hydrogen capture by the PAH may not be all that critical.

Although the present study focused on the protonated product of a neutral PAH, the parent ion THN⁺ is identical to that formed from the hydrogenation of the PAH cation. The present calculations described possible routes to the *m/z* 129 on the ground electronic state potential surface, with the energies required for various dissociation routes delivered either via multiple infrared photon or single visible/UV photon absorption. It is certainly appreciated that the dissociation mechanism proposed in this report for our IRMPD results may differ from dissociation initiated by absorption of visible/UV photons. More experimental work will be needed to decide this question.

Conclusions

(1) The infrared spectrum of neutral 1,2-dihydronaphthalene has been measured in an Ar matrix at 12 K and its bands assigned with the aid of density functional theory calculations (B3LYP/6-31++G(d,p)), with excellent agreement.

(2) Protonated 1,2-dihydronaphthalene was formed by electrospray ionization and its infrared multiphoton dissociation spectrum measured in a Fourier transform ion cyclotron mass spectrometer coupled to a infrared free electron laser. The *m/z* 131 trihydronaphthalene parent cation (THN⁺) dissociated along two channels yielding *m/z* 129 and 91 products in approximately a 2:1 ratio. It is argued that the *m/z* 129 channel represents the ejection of H₂, while the *m/z* 91 channel finally results in the benzyl ion and neutral C₃H₄, which may convert to the tropylium ion and propyne.

(3) Density functional calculations (B3LYP/6-31++G(d,p)) of the infrared spectra of all the possible THN⁺ isomers (1,2,*X*-THN⁺, *X* = 3–8) showed that the observed infrared action spectrum is best accounted for by 1,2,3-THN⁺, the isomer with the largest proton affinity and lowest relative energy.

(4) Portions of the ground-state potential energy surface of the 1,2,3-THN⁺ isomer have been calculated in an effort to understand the pathways to the observed dissociation products and the energy barriers associated with them. For the *m/z* 129 ion fragment channel, calculations of the H₂ removal from the three C(sp³) carbons show that the lowest energy dissociation takes place when H₂ is ejected from C3 (3.09 eV), followed by C1 (3.84 eV) and C2 (4.38 eV). The CC bond rupture reactions lead to the formation of the C₇H₇⁺ (*m/z* 91) and C₃H₄ fragments, and involve several hydrogen atom migrations on the carbon framework.

(5) A new model for the formation of H₂ in the interstellar medium is proposed involving the hydrogenation of one or more carbon atom sites in a PAH, absorption of visible or UV radiation, followed by large amplitude aliphatic HCH scissors vibrations leading to formation of H₂, and its subsequent ejection. Adjacent aliphatic hydrogens may then migrate to the bare ejection site and stabilize the remaining fragment.

Acknowledgment. M.V. and J.S. gratefully acknowledge the support of the Petroleum Research Foundation, administered by the American Chemical Society, for its support of this research. J.O. and J.D.S. thank the Nederlandse Organisatie voor Wetenschappelijk Onderzoek for support. The authors also thank the staff of the FELIX free electron laser facility for its skillful assistance.

Supporting Information Available: Complete ref 31. This material is available free of charge via the Internet at <http://pubs.acs.org>.

JA808965X